Multi band integration on the cyclostationary bivariable methods for bearing diagnostics.

Alexandre Mauricio, Konstantinos Gryllias

Multi band integration on the cyclostationary bivariable methods for bearing diagnostics.

Alexandre MAURICIO[1,2], Konstantinos GRYLLIAS[1,2]

[1]KU Leuven, Faculty of Engineering Science, Department of Mechanical Engineering, Division PMA, Celestijnenlaan 300 B, B-3001, Heverlee, Belgium

[2]Dynamics of Mechanical and Mechatronic Systems, Flanders Make
alex.ricardomauricio@kuleuven.be

Abstract

Rolling element bearings are critical parts of rotating machinery, as they support the loads applied to the rotating components. Therefore, continuous monitoring of the health state of the operational bearings is applied in order to detect early damages before any unexpected breakdown of the rotating machinery occurs. Bearing diagnostics is a field of intensive research, focusing nowadays mainly in complicated machinery (e.g. planetary gearboxes, multi-stage gearboxes, etc.) operating under varying conditions (e.g. varying speed and load), as they still provide challenges in terms of accuracy and time of detection/diagnosis. One of the most common methods for bearings diagnostics is the Envelope Analysis. A filter is usually applied around an excited frequency band (by impulsive damage) and the signal is enveloped, thus obtaining the Squared Envelope Spectrum. For the detection of the filtering frequency band, several band selection tools have been proposed in the past that extract the optimal band in a semi-autonomous or fully autonomous manner. The most widely used tool for band selection is the Kurtogram, where the band that returns the highest Spectral Kurtosis value is selected as the optimal band for demodulation. However, as the bearing damage may excite several frequency bands simultaneously, band-pass filtering around only one frequency band may not be sufficient for the detection of the bearing fault under the presence of noise. One proposed method to circumvent this case is to filter around several bands that carry the Signal of Interest (bearing damage signature). Recently, multi-band filtering based on the Autogram feature values, used as a pre-step in order to extract the Combined Squared Envelope Spectrum (CSES) has been presented, providing better detection performance of faulty bearings compared to the extraction of the SES after filtering over a single optimal band returned by the Autogram. Recently, a particular interest had been target to the Cyclic Spectral Correlation (CSC) and to the derived methods, due to their effectiveness in describing second-order cyclostationary signals. One of such methods is the Cyclic Spectral Coherence (CSCoh) which is a normalized version of the CSC bivariable map. Both methods are represented in the frequency-frequency domain. It has been shown that the integration of the bivariable functions over discrete spectral frequency bands is analogous to band-pass filtering. The IESFOgram has been proposed as a band selection tool, based on either the CSC or CSCoh, in order to extract the optimal frequency band. The integration on the frequency band of the bivariable map further enhances the detectability of faulty bearings on the resulting Improved Envelope Spectrum (IES). However, the method has been proposed with the integration of one single band. In this paper the method is extended towards the extraction of the Combined Improved Envelope Spectrum (CIES), performing a multi-band integration of the bivariable map around multiple resonant frequencies that are carriers of the bearing damage signature. The proposed method is applied, tested and evaluated on experimental data and the results are compared with other state-of-the-art band-selection tools.

1 Introduction

Rolling element bearings are critical components of rotating machinery and their failure can cause sudden breakdown of the system, leading to time-loss and increased costs. Condition monitoring is the field where rotating machinery is analysed, including bearings and gears and damages that may be present on the structures can be detected. Therefore, maintenance and faulty component repair can be performed before breakdown. The

diagnostics of bearings continues to be a challenge however, as their signatures are usually masked under noise and other stronger component signatures (e.g. gears). Specifically, condition monitoring of complex machinery has seen increased research, due to their wide application on critical mechanisms and to their high difficulty to diagnose caused by their many components signatures.

One of the most well established methods is the Envelope Analysis, where the signal is demodulated after band-pass filtering around the resonant frequencies excited by the damage impulses, obtaining in the end a filtered Squared Envelope Spectrum (SES). The main idea is to obtain an optimal filter band which presents a high Signal-to-Noise ratio (SNR) leading to a SES after demodulation where the fault harmonics are enhanced [1, 2]. The selection of this frequency band for demodulation is a frequency and continuous topic present in the field. The main reason is because some sort filtering processing is common to most of condition monitoring applications, and the band can either be selected by engineering knowledge, or by a methodology that selects the band in a (semi-)automated manner. The most widely used of these band selections tools is the Fast Kurtogram (FK) [3], which is an automated band selection tool based on the maximum kurtosis level. Aside from this tool there are other band selection tools that have been developed to obtain the SES. The Optimised Spectral Kurtosis (OSK) [4] selects the band with the maximum kurtosis as well, while retaining a narrow bandwidth in order to by-pass electro-magnetic interference noise on the signals. The Sparsogram [5] is based on the sparsity level on different bands based on the wavelet-packet, and the Infogram is utilizes the negentropy as a feature to detect the impulsive bands of the signal for demodulation. Moshrefzadeh and Fasana proposed the Autogram [6], a tool also based on the maximum kurtosis, but unlike the FK, it is calculated from the unbiased autocorrelation of the squared envelope of the demodulated signals. Instead of a classical filter (e.g. Butterworth filter), the undecimated wavelet packet transform (MODWPT) is used instead to split the signal in a series of frequency bands. The band of the autocorrelated squared envelope with the highest Kurtosis is selected as the optimal one, and is shown to have higher diagnosis performance than other stat-of-the-art band selections tools. One conclusion of the method is that band selection tools select only one node as the optimal, and often other unused nodes may contain useful information that is negleted. As such, they introduce the concept of multi-band integration to the Autogram, where several filtered SES, corresponding to the highest kurtosis of each level, are all combined into one spectrum denominated as Combined Squared Envelope Spectrum (CSES).

The Cyclic Spectral Correlation (CSC) and the Cyclic Spectral Coherence (CSCoh) have been proposed in the last two decades as an alternative for the SES-based methods [7, 8, 9]. The main advantage of this method falls on its ability to reveal hidden periodicities of second-order cyclostationarity, like bearing signals that are masked under stronger signals. They are represented in bi-variable maps in the frequency-frequency domain, from which its spectral axis can be integrated to obtain either the Enhanced Envelope Spectrum (EES) or the Improved Envelope Spectrum (IES). These spectra, the EES and IES, have been seen to improve the detection of cyclostationary faulty signals. However, to obtain the optimal band of demodulation for the CSC or CSCoh, its bi-variable map needs to be analysed in order to select the optimal band for integration along the spectral axis. The IESFOgram [11] as been previously proposed as a band selection tool to be applied on the bi-variable maps of CSC or CSCoh, in order to take advantage of its good perfomance in extracting the cyclistationry information of the signals. It also displays a color-mapped 1/3 binary tree like the FK and is seen to provide an optimal band of integration resulting in an IES allowing the detection of the fault frequency harmonics. However, as information of the damage can be present in other bands beside the optimal band, the authors propose an approach to combine the spectra of different bands into one Combined Improved Envelope Spectrum (CIES).

The objective of this paper is the proposal of extending the IESFOgram methodolgy by adding the information of other bands into a combined spectrum, the CIES. The methodology is validated on real signals of two datasets (one with roller bearing damage under variable speed and load conditions [10] and one from a planetary gearbox with electromagnetic interference [4]). Furthermore, the performance of the methodology is compared with the band pass filtering selection based on the Fast Kurtogram-based SES and the Autogram-based CSES. Figure 1 depicts a scheme of the used methodologies. The rest of the paper is outlined as follows. In Section 2, the background theory deemed needed for the application of the proposed method is detailed. In Section 3 the proposed methodology itself is presented. In Section 4, the methodology is tested, validated and compared with state of the art methodologies. The paper closes in Section 5 with some conclusions.

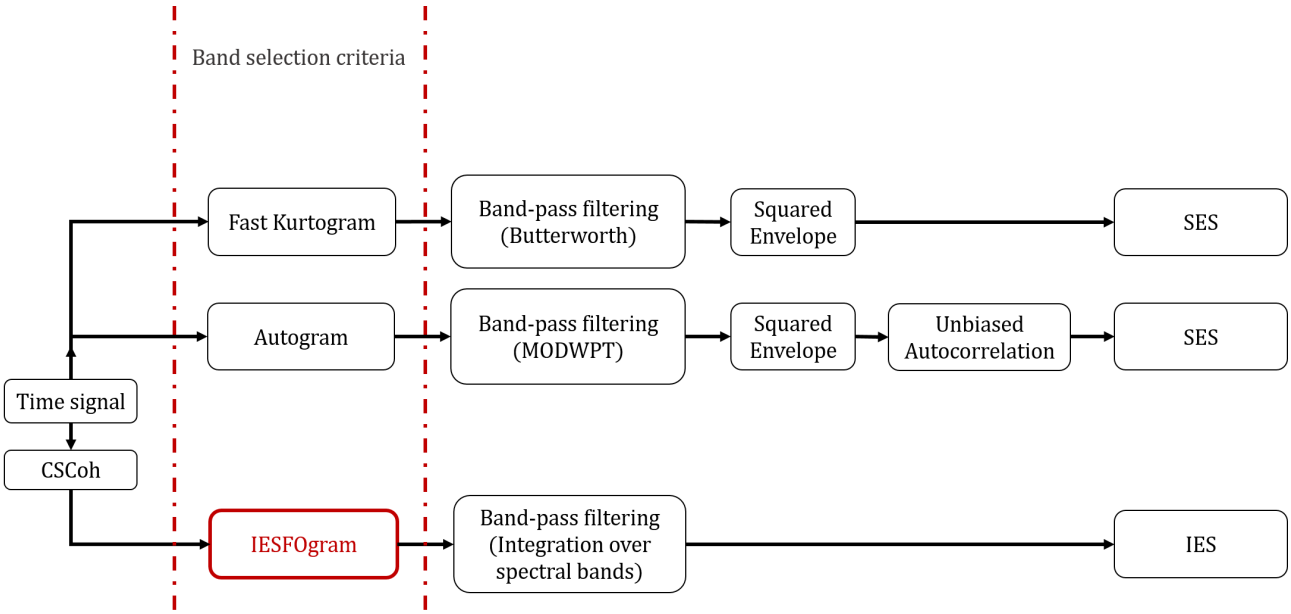

Figure 1: Schematic description of diagnostic methods based on Fast Kurtogram, Autogram, and IESFOgram

2 Cyclostationary signals

Rotating mechanical components are likely to generate cyclic transient signatures which are periodic in nature if the rotational speed is kept constant during the acquisition of signals. These signals often carry information on the health of its components, and signal processing and feature extraction are widely used in order to track the health condition of its components. Following the cyclostationary theory, the signals of interest acquired from rotating machinery can be defined into two orders of cyclostationary signals. Signals of first order of cyclostationarity (CS1) are signals whose first-order statistical moment is a periodic function of T that complies with the condition of Eq. 1.

$$C_{1x}(t) = \mathbb{E}\{x(t)\} = C_{1x}(t+T) \tag{1}$$

where $\mathbb{E}$ denotes the ensemble averaging operator, and t stands for time. In rotating machinery, CS1 vibrations signals are periodic waveforms related to components phase-locked with the rotor speed(*e.g.* shaft misalignment, spalling on meshing gears, etc). A second-order cyclostationary (CS2) signal is a signal whose second order statistical moment is periodic [13]. In particular, if its autocorrelation function is periodic with period T as described in Eq. 2.

$$C_{2x}(t,\tau) = \mathbb{E}\{x(t)x(t-\tau)^*\} = C_{2x}(t+T,\tau) \tag{2}$$

where τ corresponds to the time-lag variable. Bearing vibration signals are often described as CS2, due to having a hidden periodicity related to the shaft speed. Finally, an nth- order cyclostationary (CSn) is a signal whose nth-order statistical moment is periodic, but signal with higher order than CS2 are not taken into account, as CS1 and CS2 describe well the signals of interest generated by rotating machinery.

The Cyclic Spectral Correlation (CSC) is a tool in which the CS1 and CS2 signals are well described in the frequency-frequency domain. The method is represented as a distribution function of two frequency variable: the *cyclic frequency* α linked to the modulation; and the *spectral frequency* f linked to the carrier signal. The tool can be described also as the correlation distribution of the carrier and modulation frequencies of the signatures present in the signals, defined in Eq. 3.

$$CSC(\alpha, f) = \lim_{W\to\infty} \frac{1}{W}\mathbb{E}\{\mathscr{F}_W[x(t)]\mathscr{F}_W[x(t+\tau)]^*\} \tag{3}$$

where $\mathscr{F}_W[x(t)]$ stands the Fourier transform of the signal $x(t)$ over a finite time duration of W. Processing the CSC results in the bi-variable map which reveals the hidden modulations, making it a robust tool for

detecting the cyclostationarity in vibration signals [8, 9].

In order to minimize uneven distributions, a whitening operation can be applied to the CSC. This extended tool, named the Cyclic Spectral Coherence (CSCoh), describes the spectral correlations in normalized values between 0 and 1, and is defined as in Eq. 4 :

$$CSCoh(\alpha, f) = \frac{CSC_x(\alpha, f)}{\sqrt{CSC_x(0, f)CSC_x(0, f+\alpha)}} \tag{4}$$

Both the CSC and the CSCoh bi-variable maps can be integrated along the spectral frequency axis in order to obtain a regular spectrum, resulting in a one dimension spectrum function of the $cyclicfrequency\alpha$. The band of spectral frequencies to be integrated can be defined as the full available band, from zero to the Nyquist frequency, resulting in a spectrum that exhibits all modulations present in the signal. On the other, the band can be defined as the one that maximizes the cyclic characteristic frequency of interest while minimizing the background noise and the other frequency components that may mask the frequency of interest. In this manner, the integration over a specific band on the bi-variable map can improve the detection rate of the characteristic frequency related to the present damage on the signal. The resulting spectrum is then named Improved Envelope Spectrum (IES) and it is obtained from the frequency-frequency domain according to Eq. 5 :

$$IES(\alpha) = \frac{1}{F_2 - F_1} \int_{F_1}^{F_2} |CSCoh_x(\alpha, f)| df \tag{5}$$

3 Proposed methodology

Diagnosis using the bi-variable maps requires a deep understanding of the map in order to exploit its information. Analysis of one dimensional spectra is far more widely applied in the academia and industry and easier to anaylise. It has been seen that integration of the bi-variable function along its spectral variable results in a one dimensional spectrum, which would be a good tool on itself for diagnostics purposes. On the other hand, the diagnostics information could still be masked under the noise and other components signatures. Integration of the specific band that carries the signal of interest can further enhance the spectrum and increase the performance in the detection of the frequencies of interest. The detection of the optimal band of integration on the bi-variable map is not always straight forward.

The Improved Envelope Spectrum via Feature Optimization-gram (IESFOgram)[11] is one such band selection tool to be applied in the bi-variable map as placed in the scheme depicted Fig. 1.

The proposed method tries to optimize a Normalized Diagnostic Feature (NDF) based on the cyclic characteristics of interest (e.g. rolling element bearing characteristic fault frequencies/orders) on the demodulated spectrum resulting from the integration of the bi-variable map. The method is thought to be general enough to be applied to either the CSC or the CSCoh. The scheme representing the IESFOgram procedure and the extraction of the NDF is shown in Fig. 2, and step-by-step details for its extraction as described as follows.

Step 1: In the first step, the bi-variable map is extracted from the signal. The estimators of the $CSC(\alpha, f)$ can be based on the Averaged Cyclic Periodogram, Cyclic Modulation Spectrum or any other numerical method [14] to extract the CSC bi-variable map previously described in Eq. 3. The CSC can also be in its normalized version $CSCoh(\alpha, f)$. The user can define on its own discretion which method to use in order to obtain the bi-variable map $CSC(\alpha, f)$. The reader is forwarded to the references [15, 16], suggested as providers of the numerical implementation of the CSC in the Order-Frequency domain, and the reference [8] to the Frequency-Frequency domain CSC, if it is applied to the order tracked signal as a function of angle results in the Order-Order domain CSC.

Step 2: The next step consists in dividing the map along the spectral axis f according to the $1/3$-binary tree that is also applied to the Fast Kurtogram [3]. Each is defined by a series with a decreasing bandwidth bw and incremental steps of center frequency cf which define the upper and lower limit f_1 and f_2 described in the integration of Eq. 5. Each band is then integrated and results in a demodulated spectrum $IES_{cf,bw}(\alpha)$.

Step 3: From each processed $IES_{cf,bw}(\alpha)$, one Diagnostic Feature $DF(cf, bw)$ is extracted. This feature is based on the cyclic fault frequency/order of interest. Therefore, to calculate this feature, as well as the IESFOgram, this cyclic component needs to inserted into the method as input. The feature $DF(n)$ is defined as the sum of the N-harmonics of the characteristic fault frequency/order α_{fault} normalized by the noise level estimated in a bandwidth $2 \times f_b$, as described in Eq. 6.

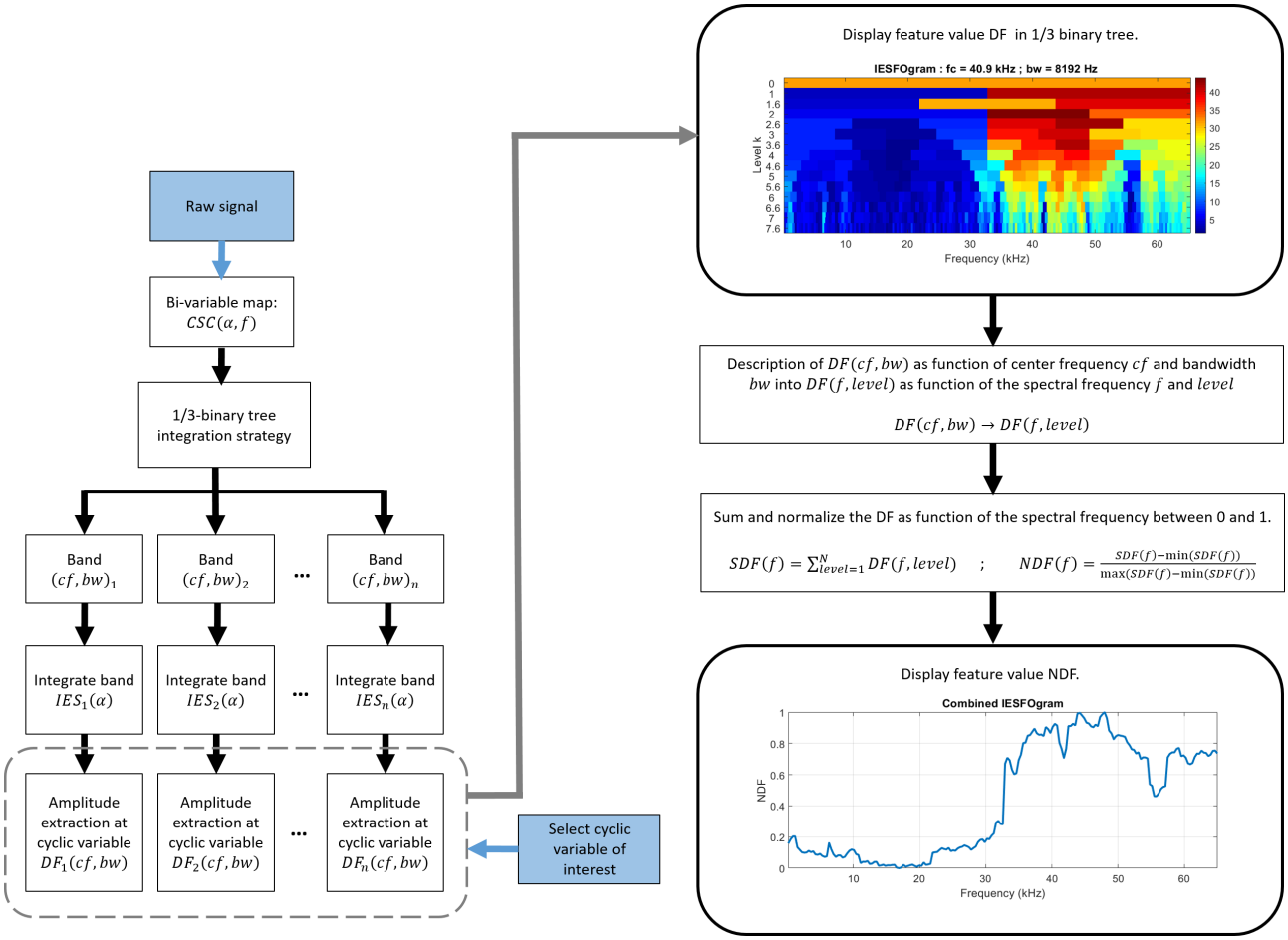

Figure 2: Schematic description of the IESFOgram procedure for extraction of CIES.

$$DF(cf, bw) = \sum_{k=1}^{N} \frac{IES_{cf,bw}(k \times \alpha_{fault})}{\frac{1}{2f_b}\left[\int_{kf_{fault}-f_b}^{kf_{fault}+f_b} IES_{cf,bw}(\alpha)d\alpha - IES_{cf,bw}(k \times \alpha_{fault})\right]} \tag{6}$$

The normalization procedure is important to be taken into account. This is due to some bands having high peak values of noise, and the direct absolute value at the fault frequencies can be higher than at the optimal band. Normalizing with the background noise level at the peaks solves this problem, making high values of the DF to correspond to bands where the frequency peaks of interest are present.

Step 4: The objective of this step is to find the the weight value to be applied on each band for integration of the bi-variable. To quantify the presence of a cyclic component in each band, the library of features $DF(cf, bw)$ is used. The higher the value of DF, the higher the presence of the component of interest is present. Thus, the optimal band OB is identified as the arguments which maximizes $DF(cf, bw)$, as described in Eq. 7.

$$OB = \underset{cf,bw}{\arg\max}[\, DF(cf, bw)\,] \tag{7}$$

Colormap presentation of the values of DF as function of (cf, bw) in a 1/3-binary tree is called the IESFOgram, and its maximum value corresponds to the selected optimal band for integration.

Step 6: The representation of $DF(cf, bw)$ as function of center frequency cf and bandwidth bw is transformed to a representation function of the spectral frequency f and the $level$, as $DF(f, level)$. To be used as a proper weight on the bi-variable map, the $DF(cf, bw)$ is summed along its level ($SDF(cf, bw)$), and then normalized between 0 and 1 ($NDF(cf, bw)$):

$$SDF(f) = \sum_{level=1}^{N} [\, DF(f, level)\,] \tag{8}$$

$$NDF(f) = \frac{SDF - min(SDF)}{max(SDF) - min(SDF)} \tag{9}$$

Step 7: The final step is to integrate the bi-variable map along the spectral axis on and weight each band with normalized diagnostic feature $NDF(f)$ in order to obtain the Combined Improved Envelope Spectrum $CIES(\alpha)$. This step can be considered not be part of the IESFOgram procedure, but as the extraction of the CIES with highest Signal-to-Noise Ratio (SNR) for diagnostic purposes.

$$CIES(\alpha) = \sum_{f=0}^{fs/2} CSCoh(\alpha, f) * NDF(f) \tag{10}$$

To define if the extracted amplitude value on the spectra of the cyclic component are statistically relevant, a threshold is also calculated, and visualized on all spectra of this paper. The threshold is the same as the one presented by the authors in [13], based on 3 times the Moving Absolute Deviation (MAD) of its spectra. The window defined on all spectra corresponds to the total number of samples of each corresponding spectrum divided by 2^7. All values above the threshold are considered to be statistically relevant for detection of the frequency.

4 Experimental application and results

In order to test and validate the proposed methodology, vibration data captured from two separate test rigs are used as case studies. One dataset corresponds to damage on the roller of a bearing under variable speed and load conditions. The second dataset corresponds vibration signals with damage in the outer race of the bearing with high electromagnetic interference present in the signals.

4.1 Case 1 - Roller damage under variable speed and load conditions

The first studied case of this paper is performed on the rolling bearing testing rig developed at the DIRG lab of Politecnico di Torino, where a high-speed spindle drives a shaft supported by a couple of identical bearings. Different damage conditions have been imposed on one of the bearings, and accelerations have been recorded in different positions and directions, under various load and speed conditions. The evaluation of the local damage on a roller has also been evaluated by monitoring the bearing under the same speed and load conditions for about 230 hours. A selection of the acquired records can be downloaded from `ftp://ftp.polito.it/people/DIRG_BearingData/` [10] .

The test rig is composed of three bearings (B1, B2 and B3) mounted inline on the output shaft of a high-speed spindle motor and a precision sledge applying radial load on the bearing on the middle, as depicted in Fig. 3.

The speed of the spindle is set through the control panel of an inverter but can not be actively controlled: not only the spindle has no keyphasor transducer or tachometer to detect its actual speed but also there is no feedback to the controller of the inverter. As a direct consequence, the actual speed of the shaft is always lower than the ideal one and the difference increases with the applied load. A static load cell allows for measuring the resulting force, whose direction is purely radial.

The main geometrical properties of the three bearings, specifically manufactured for this high speed aeronautical applications, are listed in Table 1.

Bearing reference	Pitch diameter D (*mm*)	Rollers diameter d (*mm*)	Rolling elements
*B*1 & *B*3	40.5	9.0	10
*B*2	54.0	8.0	16

Table 1: Main properties of the roller bearings [10].

The dataset corresponding to the variable conditions has 7 cases: three with indentation on the inner ring of the bearing; three with indentation on a roller of the bearing; and one with no damage (healthy). Each damage corresponds to indentation damages diameter of $450, 250$ and $150\mu m$. The case depicted in this paper

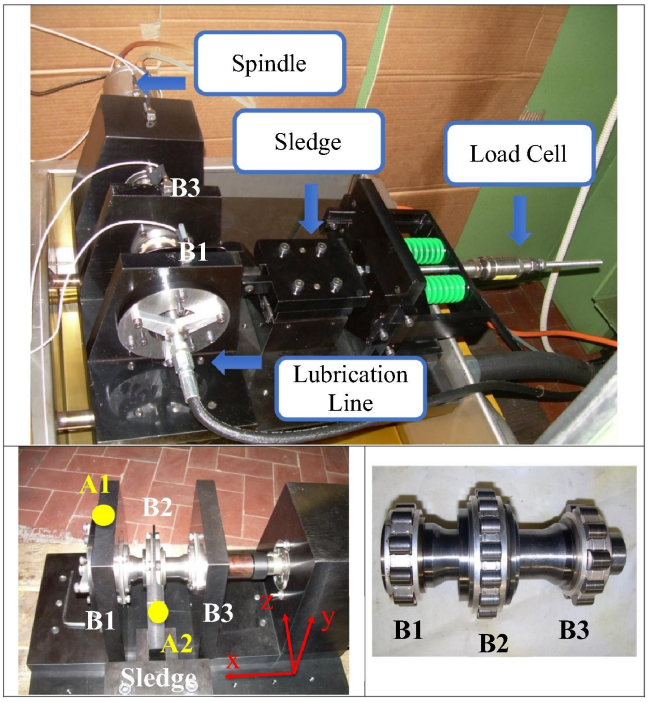

Figure 3: Test rig (up) general view, (left) position of the two accelerometers, (right) shaft with the three accelerometers [10].

corresponds to the damage on the roller with a diameter of 150μm. Each case contains signals acquired during 20 seconds at 51.2 kHz under speeds of: 100, 200, 300, 400 and 500 revolutions per second. Furthermore, the acquired signals are under 4 radial load conditions: 1000 N, 1400 N, 1800 N, and no load. The damaged bearing corresponds to bearing B1, and its characteristic frequencies under the different speed conditions are described in Table 2.

Motor speed (Hz)	FTF (Hz)	2xBSF (Hz)	BPFO (Hz)	BPFI (Hz)
100	38.9	427.8	388.9	611.1
200	77.8	855.6	777.8	1222.2
300	116.7	1283.3	1166.7	1833.3
400	155.6	1711.1	1555.6	2444.4
500	194.4	2138.9	1944.4	3055.6

Table 2: Characteristic frequencies of bearing B1 under different steady speed conditions.

From the two triaxial accelerometers, the signals used to diagnose the roller damage are on the radial direction of the accelerometer mounted on the damaged bearing B1, or in other word, the radial output of accelerometer A1 is used.

The speed reference is provided along with the signals, but the description details that the speed is in reality lower than the provided one. Upon analyzing the signal in the bivariable map from the CSCoh, it is defined that the shaft speed frequency is clear at around 90% of the theoretical one and can be extracted from the spectra under null applied load. Figure 4 shows the CSCoh map exemplifiying the clear shaft frequency at 288 Hz, for the case of speed 300 Hz and a load of 0 N.

When load is applied to the bearing, the FTF harmonics of bearing B1 become the prominent ones, as can be seen from the CSCoh map in Fig. 5 for the case of speed 300 Hz and a radial load of 1000 N.

These peaks at 90% of the given speed and the FTF were used as reference for the real speed of the test rig. With this, the frequencies at the 2xBSF can be correctly defined to determine if they are indeed present in the spectra.

The frequency at 2xBSF and its two next harmonics are then used as inputs to calculate the IESFOgram, and the weight of the different bands that will enhance the peak extraction at those frequencies, as shown in Fig. 6.

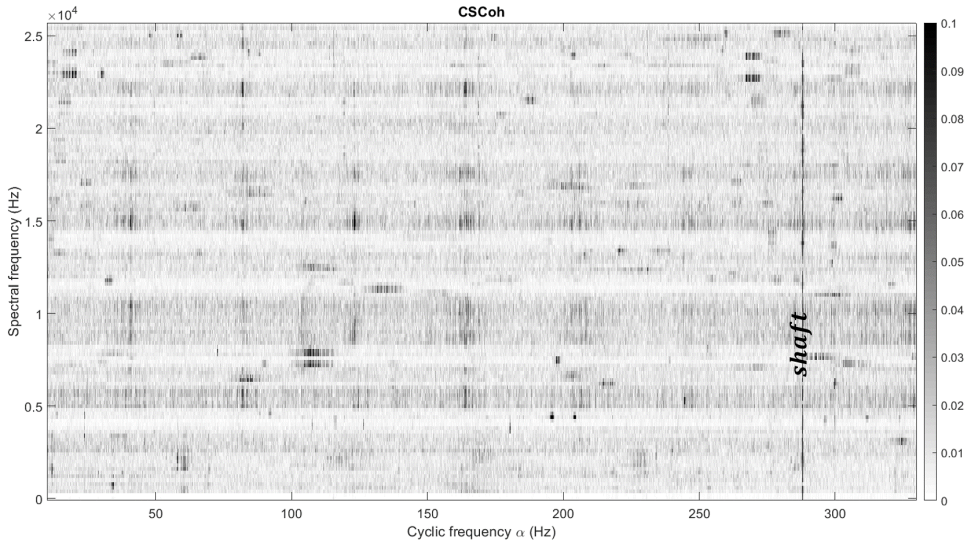

Figure 4: CSCoh bi-variable map around the first 3 FTF harmonics of the damaged bearing and shaft frequency speed of signal under no radial load.

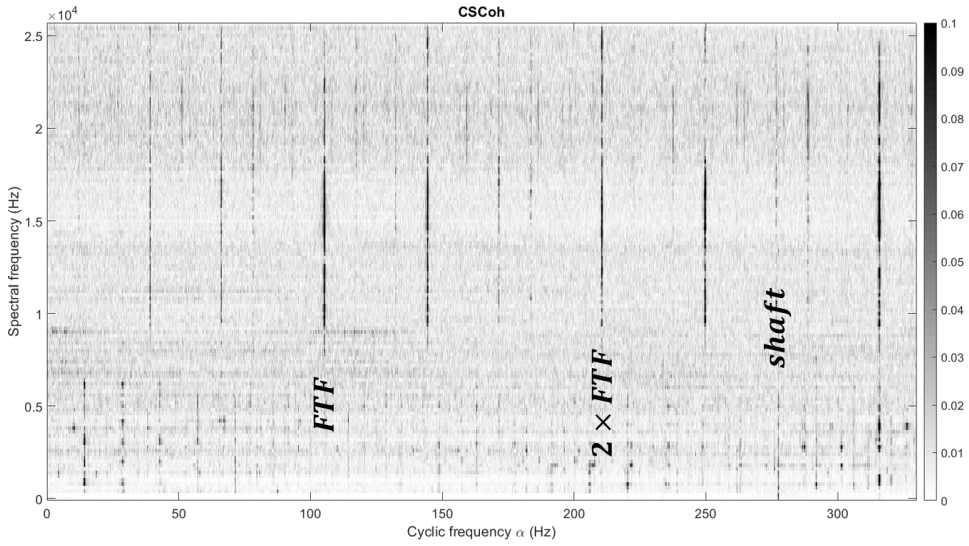

Figure 5: CSCoh bi-variable map around the first 3 FTF harmonics of the damaged bearing and shaft frequency speed of signal under 1000 N of radial load.

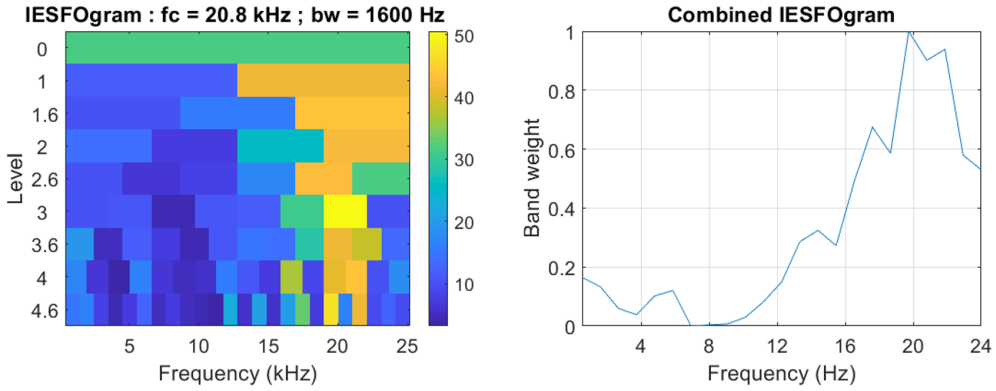

Figure 6: Signal under 300 Hz speed and 0 N load: (left) IESFOgram, (right) Combined IESFOgram.

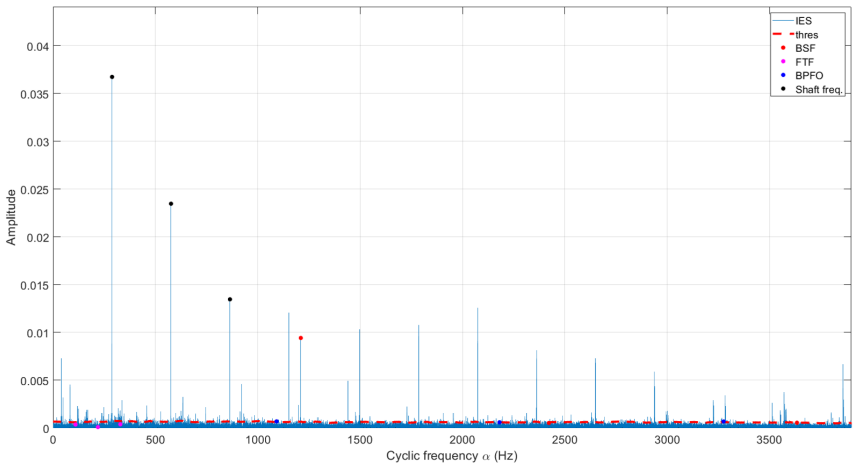

Figure 7: CIES for the signal under 300 Hz speed and 0 N load.

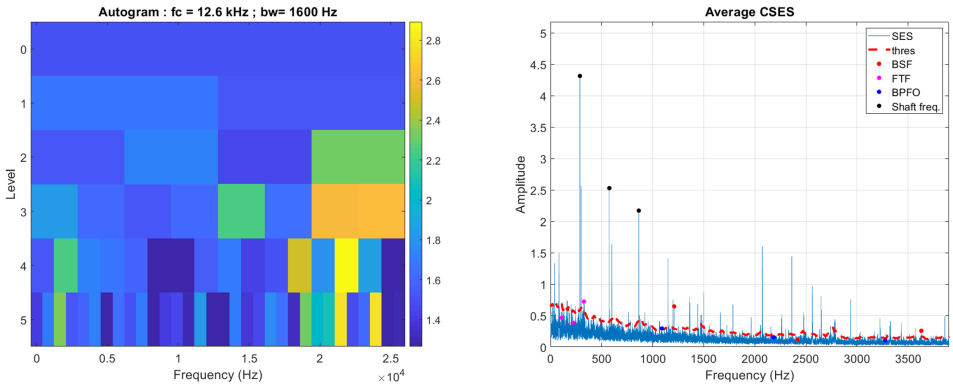

Figure 8: CSES for the signal under 300 Hz speed and 0 N load.

The IESFOgram shows high feature values at high frequencies, mainly around 20 kHz. Applying the resulting weighted function (Combined IESFOgram) to the integration of the CSCoh, the 2xBSF can be clearly extracted from the CIES seen in Fig. 7.

The Autogram applied to the same signal has a similar result, with high feature values for around high frequency bands. The Combined SES based on the Autogram is successful in extracting the peak at the 2xBSF above the threshold, along with the shaft frequency harmonics, as shown in Fig. 8.

The Fast Kurtogram detects the center frequency 10.1 kHz with a bandwidth of 1067 Hz with the highest kurtosis. The resulting SES based on the Fast Kurtogram does not provide any valuable diagnostic information, as illustrated by Fig. 9.

Following to the case of radial load of 1000 N at 300 Hz of shaft speed, the IESFOgram shows high feature values around 12 kHz. Applying the weighted function based on the IESFOgram, the 2xBSF and its harmonics are clearly detected from the Combined IES seen in Fig. 10.

For this case, the radial increases the impulses due to the roller damage, making it easier to detect the fault frequencies. The harmonics of the FTF that modulate the roller characteristic frequency also became dominant under the radial load.

The Autogram applied to the same signal has a similar result, with high feature values for around high frequency bands. The CSES based on the Autogram is also successful in extracting the peak at the 2xBSF above the threshold, as well as the FTF harmonics, as shown in Fig. 11.

In the cases with high load applied, the FTF and 2xBSF harmonics are so dominant on the signals that both the FK-based SES as well as the classical SES with no filtering detect these above the threshold. As a final remark, for the other speeds, the same pattern is found, where in high radial loads the damage related frequencies are dominant while in the no load cases they are masked in the noise level. For avoiding redundancy

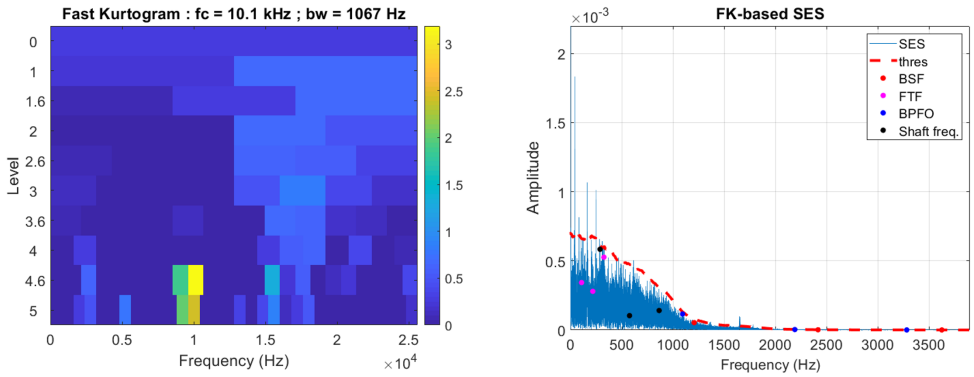

Figure 9: FK-based SES for the signal under 300 Hz speed and 0 N load.

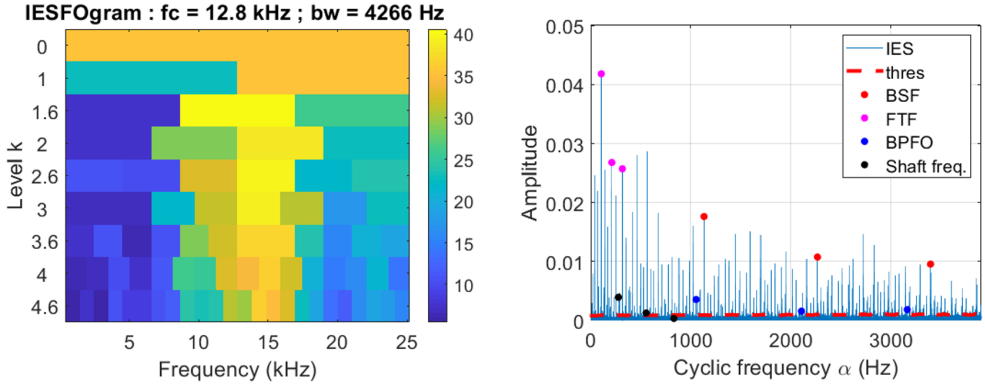

Figure 10: (left) IESFOgram and (right) CIES for the signal under 300 Hz speed and 1000 N of radial load.

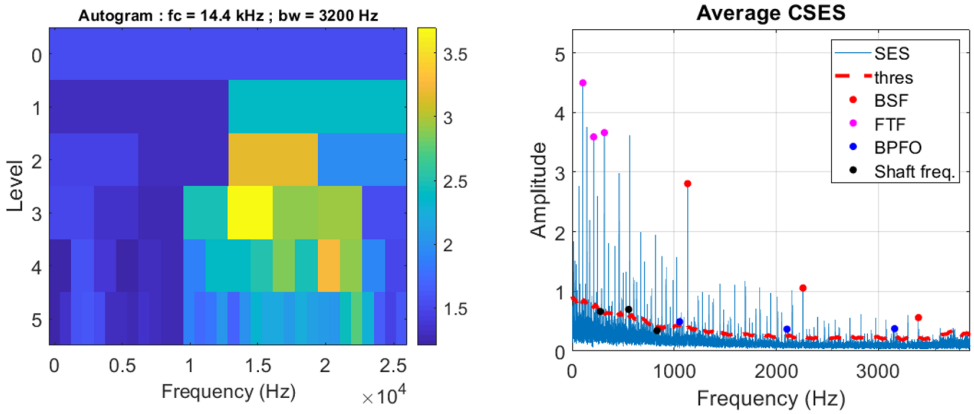

Figure 11: (left) Autogram and (right) CSES for the signal under 300 Hz speed and 1000 N of radial load.

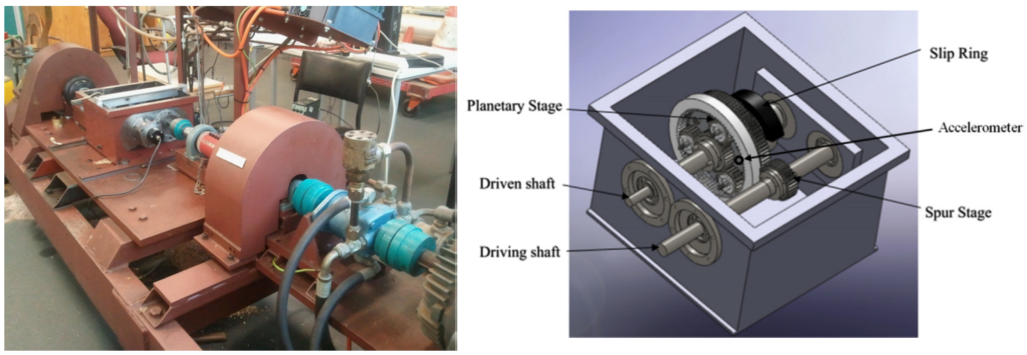

Figure 12: Test rig (left) inside view, (right) schematic representation [4].

on the results, these figure results are not shown here.

4.2 Case 2 - Outer race damage under electromagnetic interference (EMI)

The following case vibration data was acquired from the planetary gearbox test rig with applied torque is presented in Fig. 12. The gearbox torque is provided by a hydraulic system driven by a three-phase induction motor. A torque transducer is attached to measure the applied torque on the gear set while the speed of the driving shaft is controlled by a VFD. The gear ratio of the planetary stage is 1:3 (speed up) consisted of a 40 tooth sun gear, three 20 tooth planetary gears and a 80 tooth ring gear. The planet carrier is the input of the planetary stage, the sun gear is the output while the ring gear is fixed. The overall transmission ratio of the test rig is approximately 1:1 as an initial 90:32 reduction stage is attached. An accelerometer is mounted on the planet carrier to measure acceleration in the axial direction focusing towards the investigation of internal vibration measurements. The vibration signal is finally transmitted to the signal conditioner by the use of a slip ring. Faults have been seeded in the inner race and the outer races of the planet gear bearings using spark erosion. needle roller bearings are used, containing 15 rollers of 2 mm diameters and a pitch diameter of 18 mm. The depth of the faults is 0.4 mm while the width is 1.2 mm for the outer race and 1.0 mm for the inner race respectively. The measurements have been realised for each type of defect (inner and outer race) at a constant input shaft speed of 6 Hz for three torque loads 30, 50 and 70 Nm. The sampling frequency has been selected equal to 131,072 Hz, the switching frequency of the VFD was set at 14 kHz, and the control frequency of the VFD was 24 Hz (giving a nominal 6 Hz shaft speed for the 8-pole motor). The PWM carrier and the PWM message are equal respectively to 14000 Hz and 24 Hz. Based on the geometry of the bearing and its speed, the BPFO is equal to 55 Hz and the BPFI is equal to 69 Hz, but only the BPFO case is demonstrated in this paper.

Applying the Autogram to the signal with outer race damage and with a applied torque of 50 Nm, the band with the maximum Kurtosis with center frequency of 44 kHz and a bandwidth of 2048 Hz is selected as the optimal. This is the correct band with the carrier of the outer race damage. However, the impulsive bands of the carrier of the EMI have also high values of kurtosis, and the resulting CSES shows the peaks at noise level and bellow the threshold, as shown in Fig. 13.

This is the principal obstacle in detecting bearing damage with EMI noise, as both signatures have a impulsive nature which are represented with high kurtosis. The Fast Kurtogram selects the bands related to EMI as the ones with the highest kurtosis, as it as been concluded on this signal by the authors in [4, 12]. In this case, the SES based only on one band with the maximum kurtosis level of the Autogram would provide better performance.

The IESFOgram and its CIES are presented in Fig. 14, and the peaks of the BPFO are seen to be detect with clarity, well above the threshold. The case of BPFI not shown here the IESFOgram extracts the peaks of BPFI, however the CSES version also allows detection of fault.

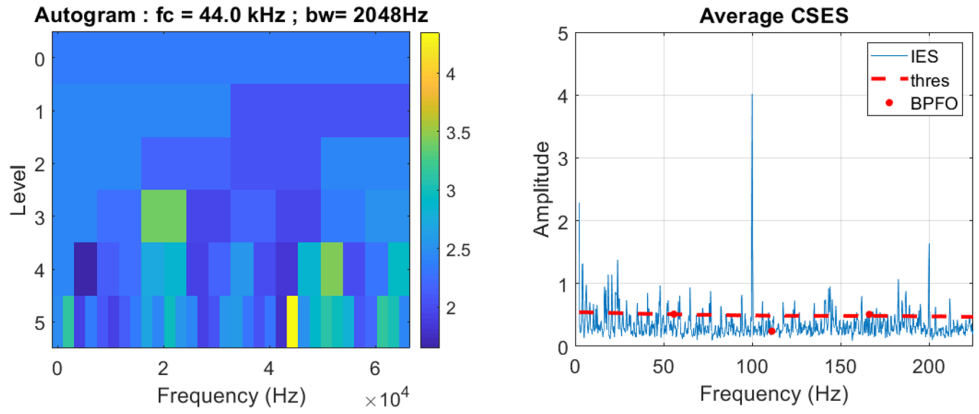

Figure 13: (left) Autogram and (right) CSES for the signal under 50 Nm of torque.

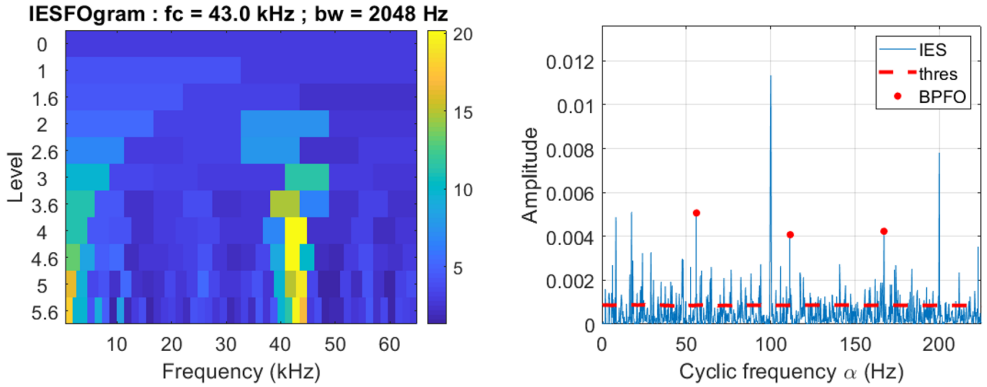

Figure 14: (left) IESFOgram and (right) CIES for the signal under 50 Nm of torque.

5 Conclusion

This paper proposes a new method for demodulation on multi-bands of frequencies using the bi-variable maps based on the Cyclic Spectral Correlation and Coherence. Initially, the IESFOgram related to the damaged bearing characteristic frequency is calculated in order to extract the spectral frequency bands that have high information content on the fault. The Normalized Diagnostic Feature as a function of frequency is defined as the normalized sum of feature values of the IESFOgram. The last step is to perform a multi band integration with the enhanced bands with high Normalized Diagnostic Feature values, and finally obtaining the Combined Improved Envelope Spectrum that allows a correct bearing diagnosis.

The methodology shows good performance in detecting the characteristic frequencies when they are present on the signals, by enhancing the bands with more relevant information on the fault and performing a multi band integration with higher weigthed values on those bands. The method was compared mainly with the Combined Squared Envelope Spectrum based on the Autogram, which also showed higher performance than the Fast Kurtogram on the detection of the bearing characteristic frequencies by also performing a multi band filtering procedure. When the signals contain a high impulsive signal with the same nature as a bearing damage, such as electromagnetic interference, the CSES-based on the Autogram shows to keep the peak frequencies of interest bellow the noise level in case of high impulsive noise spread over several bands. The CIES shows to be able to extract clearly the fault frequency peaks above the noise level while ignoring the bands dominated by the impulsive noise. This is shown to be the case because the IESFOgram is targeted at the frequencies of interest, while the Autogram is blind. Indeed, the main disadvantage of the IESFOgram compared to the Autogram and the Fast Kurtogram is that it is not a blind method.

The methology was tested and validated on two experimental datasets: the first under variable speed and load condition, and the second on signals with high electromagnetic interference contamination. The results show the method can diagnose with confidence bearing damages on vibration signals.

Acknowledgements

The authors would like to thank Ali Moshrefzadeh and Alessandro Fasana for the sharing the roller bearing damage vibration data and the Autogram publicly, Jerome Antoni for sharing the Fast Kurtogram publicly, and Wade Smith and Robert Randall for providing vibration signals with electromagnetic interference. K. Gryllias gratefully acknowledges the Research Fund KU Leuven.

References

[1] Randall, R., Antoni, J., *Rolling Element Bearing Diagnostics - A Tutorial*, Mechanical Systems and Signal Processing, 2012, pp.485-520 (25).

[2] Feldman, M., *Hilbert transform applications in mechanical vibration*, John Wiley and Sons, 2011.

[3] Antoni, J., *Fast computation of the kurtogram for the detection of transient faults*, Mechanical Systems and Signal Processing, 2007, pp.108-124 (21).

[4] Smith, W., Fan, Z., Pheng, Z., Li, H., Randall, R., *Optimised Spectral Kurtosis for bearing diagnostics under electromagnetic interference*, Mechanical Systems and Signal Processing, 2016, pp.371-394 (75).

[5] Tse, P. W., *The sparsogram: A new and effective method for extracting bearing fault features*, Prognostics and System Health Managment Confernece, 2011, pp.1-10).

[6] Moshrefzadeh, A., Fasana, A., *The Autogram: An effective approach for selecting optimal demodulation band in rolling element bearings diagnosis*, Mechanical Systems and Signal Processing, 2017, pp.294-318 (105).

[7] Randall, R., Antoni, J., Chobsaard, S., *The relationship between spectral correlation and envelope analysis in the diagnostics of bearing faults and other cyclostationary machine signals*, Mechanical Systems and Signal Processing, 2001, pp.945-962 (15).

[8] Antoni, J., Xin, G., Hamzaoui, N., *Fast computation of the spectral correlation*, Mechanical Systems and Signal Processing, 2017, pp.248-277 (92).

[9] Antoni, J., *Cyclic spectral analysis in practice*, Mechanical Systems and Signal Processing, 2007, pp.597-630 (21).

[10] Daga, A. P., Fasana, A., Marchesiello, S., Garibaldi, L., *The Politecnico di Torino rolling bearing test rig: Description and analysis of open access data*, Mechanical Systems and Signal Processing, 2019, pp.252-273 (120).

[11] Mauricio, A., Smith, W., Qi, J., Randall, R., Gryllias, K., *Cyclo-non-stationarity based bearings diagnostics of planetary bearings*, CMMNO, Santander, Spain, 2018, pp.1-10.

[12] Mauricio, A., Qi, J., Sarrazin, M., Janssens, K., Smith, W., Randall, R., Gryllias, K., *Cyclostationary-based bearing diagnostics under electromagnetic interference*, ICSV25, Hiroshima, Japan, 2018, pp.1-8.

[13] Antoni, J., Bonnardot, F., Raad, A., El Badaoui, M., *Cyclostationary modelling of rotating machine vibration signals*, Mechanical Systems and Signal Processing, 2004, pp.1285-1314 (18).

[14] Borghesani, P., Antoni, J., *A faster algorithm for the calculation of the fast spectral correlation*, Mechanical Systems and Signal Processing, 2018, pp.113-118 (111).

[15] Abboud, D., Baudin, S., Antoni, J., Remond, D., Eltabach, M., Sauvage, O., *The spectral analysis of cyclo-non-stationary signals*, Mechanical Systems and Signal Processing, 2016, pp.280-300 (75).

[16] Abboud, D., Antoni, J., *Order-frequency analysis of machine signals*, Mechanical Systems and Signal Processing, 2017, pp.229-258 (87).